

# Simulation of soil organic carbon potential sequestration for high Andes Peruvian croplands

Carlos Carbajal<sup>(1)\*</sup> , Jesús Vera<sup>(2)</sup> , Samuel Pizarro<sup>(2)</sup>  and Carlos Mestanza<sup>(3)</sup> 

<sup>(1)</sup> Instituto Nacional de Innovación Agraria, Dirección de Servicios Estratégicos Agrarios y Monitoreo en las Estaciones Experimentales Agrarias, La Molina, Lima, Perú.

<sup>(2)</sup> Instituto Nacional de Innovación Agraria, Dirección de Servicios Estratégicos Agrarios y Monitoreo en las Estaciones Experimentales Agrarias, El Tambo, Junín, Perú.

<sup>(3)</sup> Universidad Nacional Agraria La Molina, La Molina, Lima, Perú.

**ABSTRACT:** Soil organic carbon (SOC) sequestration in croplands represents a significant opportunity to mitigate climate change by removing carbon dioxide from the atmosphere. Simulation tools are increasingly used to assess the impact of climate change and soil management on soil organic carbon stock dynamics. Although Andean soils typically store large amounts of organic carbon, agricultural practices, especially plowing, may deplete these stocks, creating a need to understand these dynamics better. Here, we show the soil organic carbon sequestration potential in croplands in the Peruvian Andean region over 50 years. Soil organic carbon content and bulk density were spatially predicted across the study area using 100 georeferenced soil samples to quantify organic carbon stocks. Spatial interpolation was performed using Ordinary Kriging with exponential and spherical variogram models, which provided the best fit to the data. The RothC model was used to simulate changes in soil organic carbon stocks under two contrasting agricultural management scenarios: one without manure application and another with annual application of one ton of manure per hectare. We found that manure application can substantially increase soil organic carbon sequestration in croplands with increases ranging from 105.22 to 214.94 Mg ha<sup>-1</sup> over 50 years. The potential for increased carbon sequestration through manure application could help compensate for losses in other areas of the watershed, particularly grasslands (74.4 % of the area). This study contributes valuable information for developing sustainable land management strategies in Andean agroecosystems.

**Keywords:** soil organic carbon, RothC model, SoilR, geostatistics, pedometrics.

\* **Corresponding author:**  
E-mail: cmcarbajal@gmail.com

**Received:** December 21, 2024

**Approved:** March 05, 2025

**How to cite:** Carbajal C, Vera J, Pizarro S, Mestanza C. Simulation of soil organic carbon potential sequestration for high Andes Peruvian croplands. Rev Bras Cienc Solo. 2025;49:e0240241. <https://doi.org/10.36783/18069657rbc20240241>

**Editors:** José Miguel Reichert  and João Tavares Filho .

**Copyright:** This is an open-access article distributed under the terms of the Creative Commons Attribution License, which permits unrestricted use, distribution, and reproduction in any medium, provided that the original author and source are credited.



## INTRODUCTION

Soil is a natural body that possesses a significant capacity to store atmospheric carbon in organic forms, thereby serving as a means to mitigate climate change (McBratney et al., 2014). Soil organic carbon (SOC) determines soil health and fertility, is highly related to vegetation productivity, and improves soil structure by increasing water holding capacity and soil nutrients. Soil contains up to 3 times more SOC than the atmosphere and vegetation, and a change in soil carbon sequestration rate drastically impacts the carbon cycle and climate regulation (Ramesh et al., 2019). The initiative “4 per 1000” shows that an annual growth rate of 0.4 % of global soil organic carbon stocks would potentially stabilize the increase in atmospheric CO<sub>2</sub> (Rumpel et al., 2020).

Agriculture is an activity that leads to soil degradation; more than 50 % of agricultural soils are moderately or highly degraded (Nachshon, 2020). Soil formation process is slow, and technically, they are non-renewable, but soil fertility can be restored by rebuilding the organic carbon concentrations in the remaining topsoil (Bradford et al., 2019). Establishing a recalcitrant soil organic carbon pool by implementing effective agricultural practices for long-term sequestration can potentially sequester 80–130 GT of carbon (Siddique et al., 2024). Under the climate change scenario, increasing soil organic carbon stock in croplands is a considerable challenge; before considering the accumulation of organic carbon, it is crucial to address the losses of soil organic carbon that have occurred (Riggers et al., 2021). Therefore, monitoring SOC requires mapping the content of the target area and performing future estimations.

Geostatistical methods and machine learning are widely used to map soil properties based on satellite information (Mousavi et al., 2023). Time prediction models, such as RothC, are used to estimate changes over specific periods (Lin et al., 2024). These tools were used to estimate a carbon sequestration potential of 2.13 kg m<sup>-2</sup> in the top 0.20 m of croplands in China (Wang et al., 2023). Studies indicate that Andean soils respond positively to management practices like fallow, crop rotation, and terraces (Alavi-Murillo et al., 2022). Despite existing research on the spatial distribution of soil organic carbon in the South American Andes (Canaza et al., 2023), a significant knowledge gap remains regarding temporal SOC dynamics. Existing Andean region studies addressing this issue are limited to the tropical zone (Diaz et al., 2023; Avadí, 2023) and thus do not apply to high-altitude agroecosystems.

To address this knowledge gap and understand the spatial and temporal changes in soil organic carbon sequestration in Andean agroecosystem, we proposed to estimate SOC stocks in the Upper Mantaro Basin and model the evolution of carbon sequestration as a function of agricultural management and climate change.

## MATERIALS AND METHODS

### Description of study area

The Alto Mantaro sub-basin is located in the Peruvian Andes (11° 46' 40" S, 75° 26' 40" W, WGS84) and covers approximately 2,114.82 km<sup>2</sup> (Figure 1), with elevations between 3,186 and 5,141 m above sea level. According to the Thornthwaite climate classification map of Peru (Castro et al., 2021), the lower zones boast a semi-dry and temperate climate characterized by consistent humidity throughout the year. Once the altitude surpasses 4,500 m a.s.l., the climate shifts to a rainy and cold one, and there is a lack of humidity during the autumn and winter months. Sub-basin encompasses the Mantaro Valley, an important agricultural area in the Junín region of Peru, with croplands between 3,000 to 3,400 m a.s.l. on the alluvial terraces along the Mantaro River in the provinces of Jauja, Huancayo, Concepción, and Chupaca (Cuellar-Bautista and Medina-Hinostroza, 2009). According to the World Reference Base for Soil Resources (IUSS Working Group WRB, 2007), the study area was dominated in order of extension by Cambisols, Luvisols, Phaeozems, and Andosols soil classes.

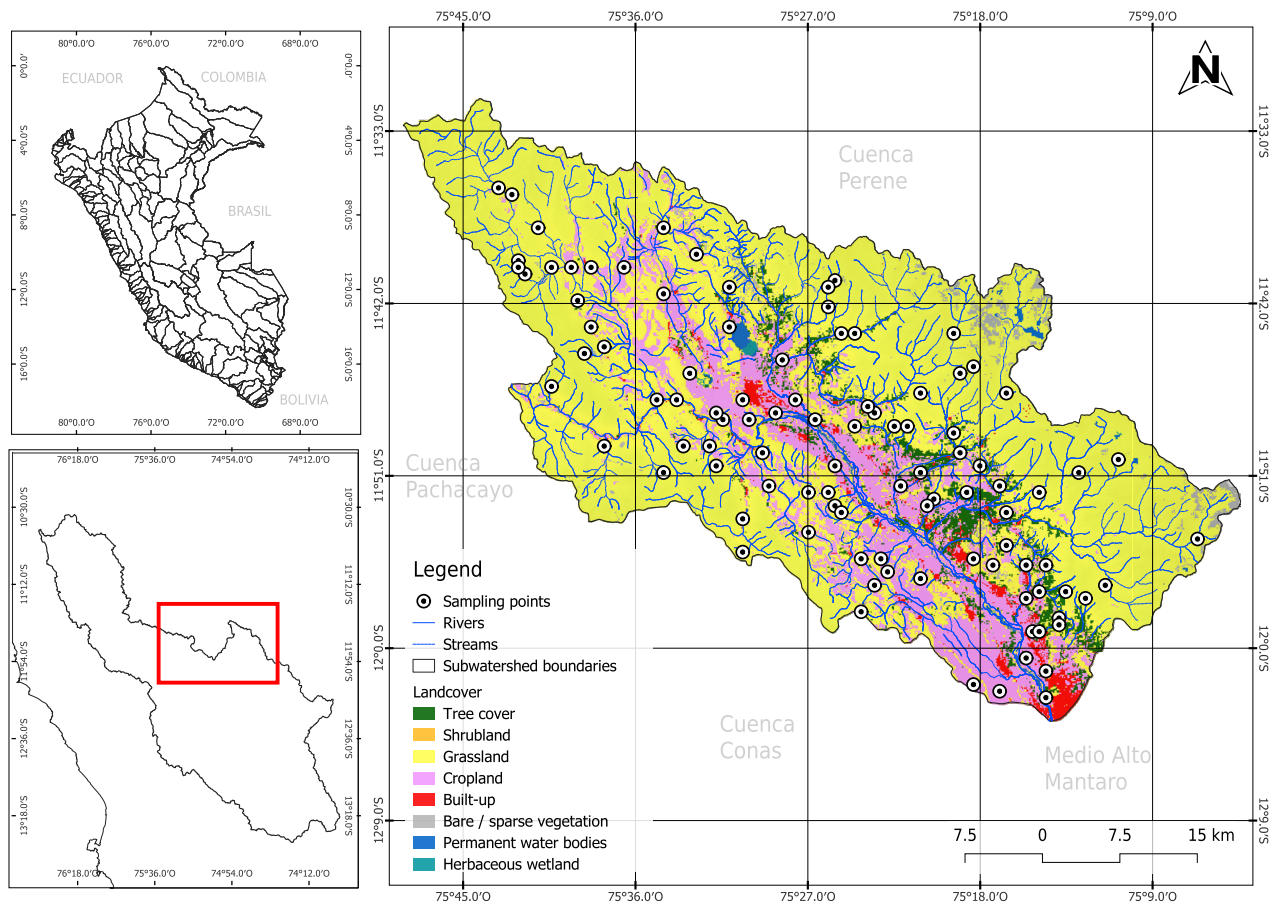


**Figure 1.** Soil sampling distribution and location of the Mantaro basin. Landcover (colored surface) and hydrology (blue lines) are shown within the geographic boundaries.

### Soil sampling and analysis

Sampling points were selected using a conditioned Latin hypercube (cLHS) algorithm that generated 100 sampling points (Figure 1). The cLHS method is a stratified random procedure that selects samples based on the covariate distributions. It uses an optimization routine, minimizing an energy function that describes how well the candidate sampling scheme represents a Latin hypercube of covariate distributions (Roudier et al., 2012). We acquired the generation of points by employing the `clhs` package in R (Roudier, 2011); they are supported by the `raster` (Hijmans, 2024) and `rgdal` (Bivand et al., 2023) packages. The `clhs` package enabled us to have flexibility in sampling location by utilizing the “`similarity_buffer`” function to compute the Gower similarity index (Gower, 1971). As a data source, we considered incorporating a set of covariates generated with the support of the SAGA tools (Conrad et al., 2015) and Google Earth Engine (GEE).

A disrupted sample was obtained from 0 to 0.30 m depth at every sampling location, and an undisturbed sample at a depth of 0.15 m using a metallic cylinder. Laboratory analyses were performed in the Soil, Water, and Foliar Laboratory (LABSAF) of the La Molina Agrarian Experimental Station (EEA). Soil organic carbon (SOC) was determined by dry combustion (ISO, 1996) using an elementary analyzer LECO CN828 (Leco Corp., St. Joseph, MI, USA), and dry bulk density (BD) was determined using the core method (ISO, 2017).

### Soil mapping

Inside the Python ecosystem, we used a geostatistical approach to map soil properties, such as bulk density (BD) and soil organic carbon (SOC). They are evaluated with power,

gaussian, spherical, and exponential models using the Pykrige library (Murphy, 2024) in Python language version 3.12.3 (Van Rossum and Drake Jr, 1995). We chose the variogram models mentioned, considering the root mean square error (RMSE) and coefficient of determination ( $R^2$ ) metric values implemented in code with “sklearn.metrics” module from the scikit-learn library (Pedregosa et al., 2011). Surface maps were interpolated utilizing Ordinary Kriging (OK) to generate raster maps with a pixel size of 100 m.

### Description of soil modeling with RothC

Prediction of soil carbon sequestration scenarios was carried out with the RothC model (Coleman and Jenkinson, 1996) executed by the SoilR package (Sierra et al., 2014) in R software version 4.2.3 (R Development Core Team, 2023). RothC is a Soil Organic Matter (SOM) turnover model and was developed to simulate changes in SOC stocks in arable topsoils from the Rothamsted Long-term Field Experiments in the UK (Zimmermann et al., 2007); the model includes the effects of soil type, temperature, moisture content, and plant cover, with a monthly time step (FAO, 2022).

### Soil and climate inputs

Initial soil organic carbon stock (STOCK) was calculated using equation 1, in which soil mass was determined by multiplying soil volume ( $10,000 \text{ m}^2 \times 0.30 \text{ m depth}$ ) by bulk density (BD), and then STOCK was derived using soil organic carbon content (SOC).

$$\text{STOCK (Mg ha}^{-1}\text{)} = 3000 \times \text{BD} \times \text{SOC} \quad \text{Eq. 1}$$

A list of raster layers conforms to part of the input requirements of the model, monthly averages of climatic variables like temperature, precipitation, and potential evapotranspiration (ET), the two first we get from WorldClim 2 database (Fick and Hijmans, 2017) and ET from Version 3 of the Global Aridity Index and Potential Evapotranspiration Database based upon the FAO Penman-Monteith Reference Evapotranspiration equation (Zomer et al., 2022), besides variables like percent clay content from Soilgrids system at 250 m resolution (Hengl et al., 2017) and annual litter inputs; for the last one, we used net primary production (NPP) get from MODIS images database (Running and Zhao, 2021) at 500 m pixel resolution, accessing data with the support of Google Earth Engine (GEE) platform. Another input requirement indicated in centimeter units is soil thickness, assuming it is an organic layer of topsoil.

### Land cover and soil management data

The ESA WorldCover 2021 v200 product (Zanaga et al., 2022) was considered for a spatial modeling approach to identify land use management data. It was then aligned with their Land Cover classes aggregation and reclassification scheme to FAO land cover classes and default decomposable to resistant plant material ratios (RT) (FAO, 2022). In this case, the values of the land cover classes existing in the area of study provided to the model are shown in table 1.

### Modeling future conditions and climate effects

With the model in the R language, we run simulations every ten years to reach 50 years. We create a vector of time steps corresponding to monthly times to run the simulation. Evaluating the effects of climate on decomposition was calculated using functions of the SoilR package, like “ft.RothC” for temperature effects and “fW.RothC” for moisture effects, both per month time periods (Sierra et al., 2014). Moisture model was set using potential evapotranspiration ( $pE = 1$ ) and under vegetation conditions (bare = FALSE).

**Table 1.** Decomposable-to-Resistant Plant Material (DPM/RPM) Ratios for RothC Model Parameterization, sourced from Global Soil Carbon Datasets (FAO, 2022)

ESA Land Cover Class	RT(1)
10 Tree cover	0.25
20 Shrubland	0.67
30 Grassland	0.67
40 Cropland	1.44
50 Built-up	0.01
60 Bare/sparse vegetation	0.67
70 Snow and ice	0.01
80 Permanent water bodies	0.01
90 Herbaceous wetland	1.44

<sup>(1)</sup> Ratio of Default Decomposable Material (DPM) and Resistant Plant Material (RPM).

### Initial soil organic matter pools

Model incorporates five soil organic matter pools: decomposable plant material (DPM), resistant plant material (RPM), microbial biomass (BIO), humified organic matter (HUM), and inert organic matter (IOM). The IOM pool, assumed to remain constant over time, was estimated using the model proposed by Falloon et al. (1998). The RPM, HUM, and BIOM pools were estimated using the models of Weihermüller et al. (2013). Computation of carbon allocation in each pool is determined by the amount of clay, except for IOM, as shown in the following equations 2, 3, 4 and 5.

$$\text{RPM} = (0.184 \cdot \text{SOC} + 0.1555) \cdot (\text{clay} + 1.275)^{-0.1158} \quad \text{Eq. 2}$$

$$\text{BIO} = (0.015 \cdot \text{SOC} + 0.0075) \cdot (\text{clay} + 8.8473)^{0.0567} \quad \text{Eq. 3}$$

$$\text{HUM} = (0.7148 \cdot \text{SOC} + 0.5069) \cdot (\text{clay} + 0.3421)^{0.0184} \quad \text{Eq. 4}$$

$$\text{IOM} = 0.049 \cdot \text{SOC}^{1.139} \quad \text{Eq. 5}$$

Finally, the DPM pool was calculated as shown in equation 6 by subtracting the sum of the other pools from the initial STOCK (Sierra and Müller, 2015). In cases where this resulted in a negative value, the DPM was set to 0.

$$\text{DPM} = \text{SOC} - (\text{IOM} + \text{RPM} + \text{HUM} + \text{BIO}) \quad \text{Eq. 6}$$

### Special conditions for the model RothC

To generate a SoilR Model object, we need to use the “RothCModel” function and provide the previously mentioned inputs. Once the model is initialized, we can solve the object to calculate the SOC stocks for each pool. To successfully complete this task, we must execute a loop iterative function on every pixel within the raster layers. Then, the RothC model was changed to simulate specific conditions only on cropland cover, assuming the inclusion of Farm Yard Manure (FYM) inputs at a rate of 1 Mg ha<sup>-1</sup>.

## RESULTS

### Data description

Some descriptive statistics of RothC input variables, like minimum, maximum, mean, standard deviation, and coefficient of variability, for soil organic carbon, bulk density, temperature, precipitation, clay content, potential evapotranspiration, and net primary production are presented in table 2. Climatic variables and clay content exhibit low variability ( $CV < 15\%$ ) or uniformity. Bulk density and NPP show low-to-moderate variability ( $15\% < CV < 20\%$ ), reflecting latent variability. SOC shows wide variability, showing considerable heterogeneity among high Andean croplands.

### Soil mapping

Exponential and spherical models were the best fit for soil organic carbon and bulk density. A detailed description of variogram parameters can be found in table 3. The proportion of space-dependent variance was greater for SOC (0.74) than for BD (0.41), however, both models had a good fit to the data ( $R^2 > 0.50$ ), and the prediction errors (RMSE) were small based on the scale of each variable. Soil organic carbon (30 km) and BD (13 km) range were greater than 10 km, considering the area of the study zone, the spatial structure of both variables is long range.

Spatial distribution of SOC and BD is depicted in figure 2, along with their variance values for both predicted results. Coefficient of variation maps enable the visualization of similar uncertainty patterns. High predicted SOC values are observed in the southeast, with the lowest values found in the flat zones. In contrast, the behavior of Bd values in these zones is opposite, with the highest values observed.

**Table 2.** Summary statistics of RothC input variables: Temperature (Tmp), Precipitation (Prep), Clay, Potential evapotranspiration (ETo), Bulk density (BD), Net Primary Production (NPP), and Soil Organic Carbon (SOC)

Variable	Mean	SD	Min	Max	CV
					%
Tmp (°C)	9.72	1.07	6.89	11.44	11.00
Prep (mm)	65.12	5.56	56.28	77.41	08.54
Clay (%)	30.77	1.59	25.25	32.62	05.17
ETo (mm)	115.61	3.69	104.29	120.91	03.19
BD (Mg m <sup>-3</sup> )	1.20	0.18	0.80	1.57	16.07
NPP (kg m <sup>-2</sup> )	4.65	0.92	1.95	6.38	19.78
SOC (%)	2.79	1.82	0.61	8.14	65.23/

SD: standard deviation; Min: minimum; Max: maximum; CV: coefficient of variation.

**Table 3.** Parameters of the variogram model: nugget (C0), sill (C0+C), range (Ra) in meters, proportion of spatial variability (PSV), coefficient of determination (R<sup>2</sup>), and root mean square error (RMSE) are presented. PSV was calculated as C/(C0+C)

Soil property	Model	C0	C0+C	Ra	PSV	R <sup>2</sup>	RMSE
Soil organic carbon	Exponential	1.33	5.03	30664	0.74	0.82	0.89
Bulk density	Spherical	0.02	0.03	13503	0.41	0.53	0.12

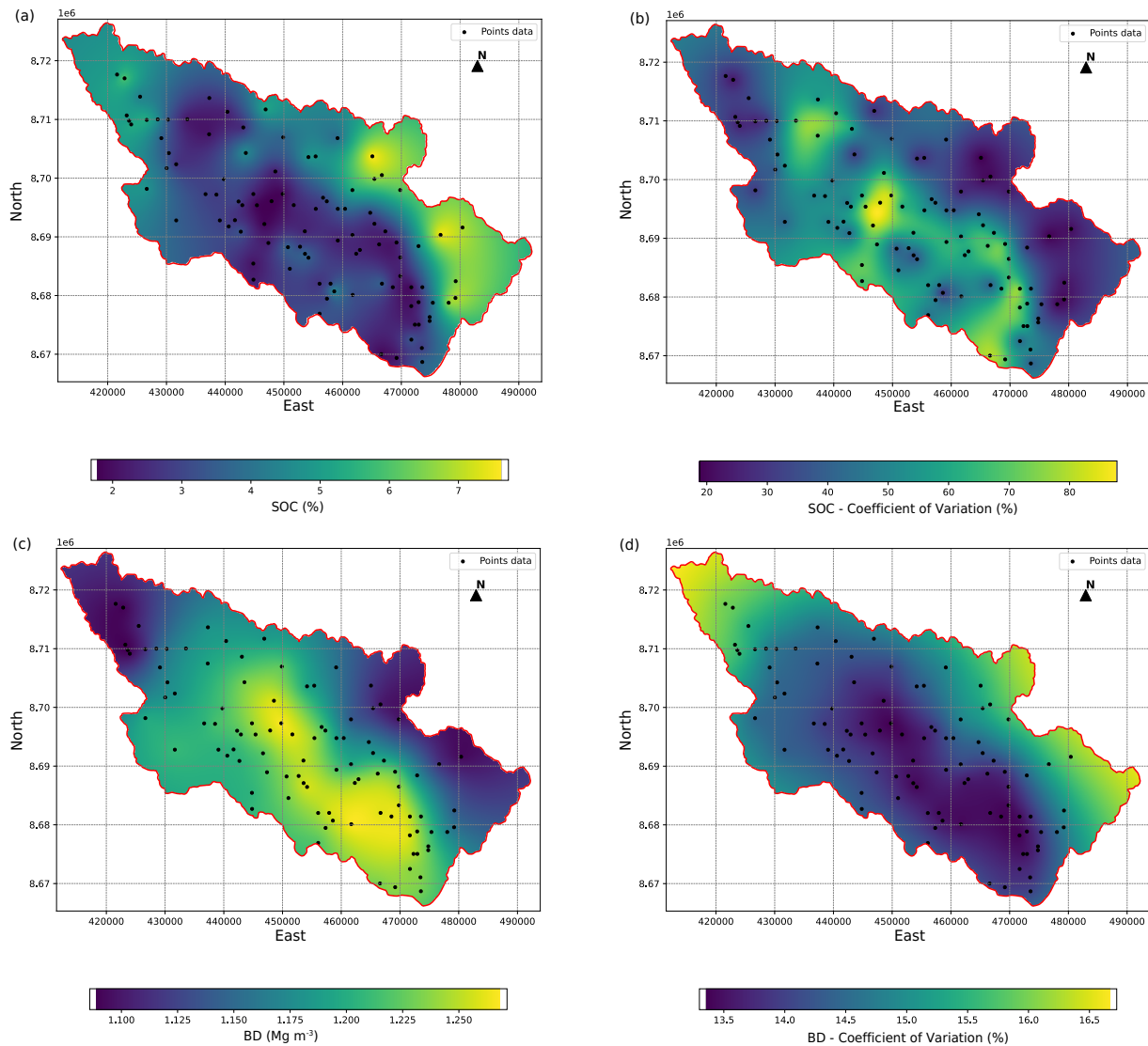


**Figure 2.** Spatial distribution maps using Ordinary Kriging (OK) interpolation method: (a) soil organic carbon (SOC); (b) coefficient of variation of SOC; (c) bulk density (BD); and (d) coefficient of variation of BD.

### Soil carbon stock sequestration forecasting

Processed data from a soil carbon model, such as RothC, is used to illustrate the spatial distribution of projected changes in accumulated pool values over a 50-year period (Figure 3). Initially, the southeastern area of the basin exhibits high values and coincides with areas where the highest altitudes occur, but as the simulation progresses, there is a noticeable drop in the average outcomes at the whole basin level. The main land cover categories were examined in table 4, revealing high values in grassland and sparse vegetation initially, in contrast to cropland and tree cover. As time advances, there is a gradual decrease in grass and sparse vegetation, while cropland and tree cover remain with slight changes.

Incorporating 1 Mg of manure into the cropland resulted in a gradual and consistent increase in the simulation results over the evaluated period. Data in table 4 shows a significant rise in profit values, reaching up to 100 Mg per hectare approximately after the simulation of the initial 10-year period. Following this, there is a steady increment of around 3 Mg every 10 years. The findings show that by applying 1 ton, the losses of organic carbon in grassland can be mitigated, as losses are observed within the range of 11 tons during this timeframe. We appreciate that the size of grassland areas is significantly greater than that of cropland areas.

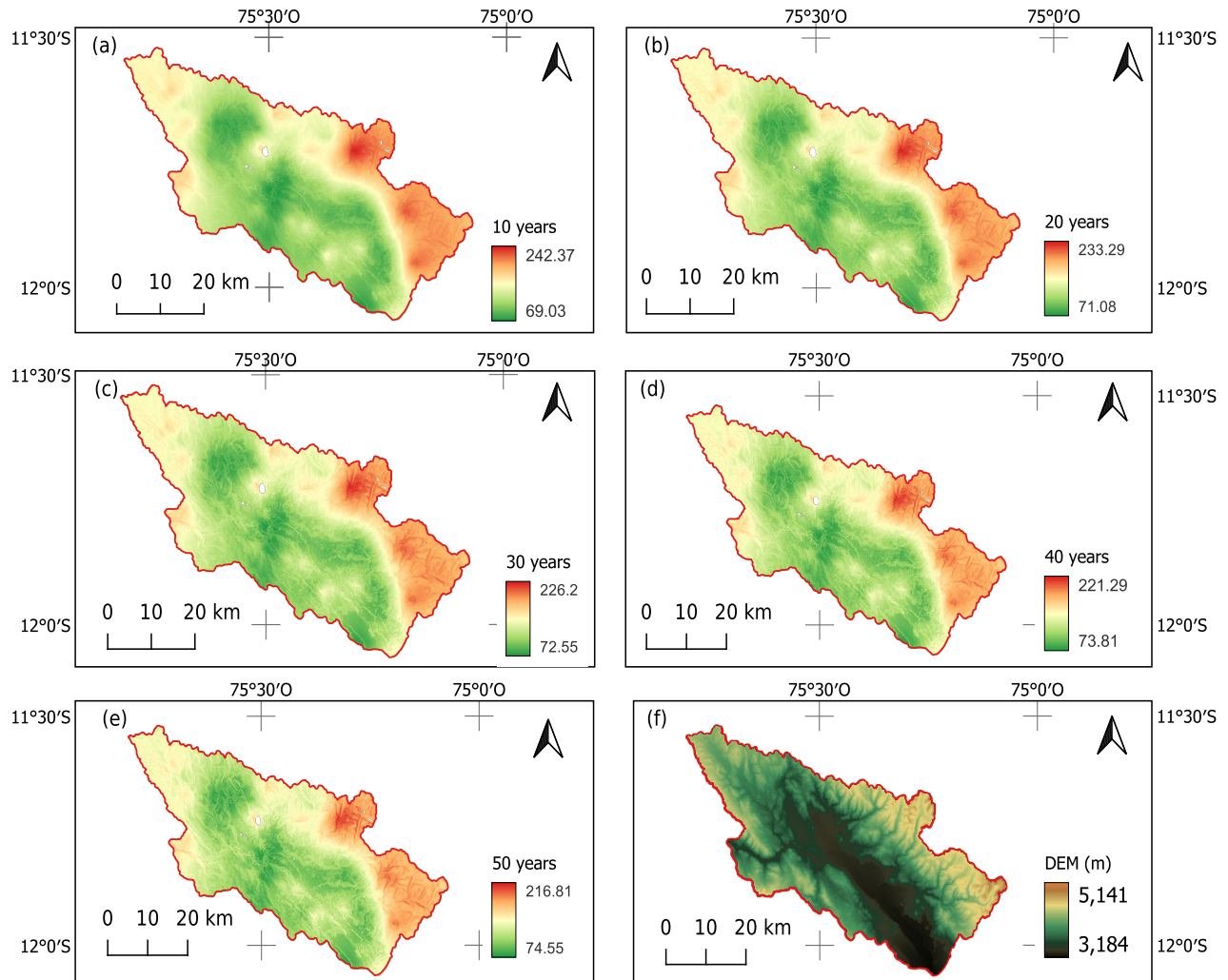


**Figure 3.** Spatial distribution of soil carbon stock using the RothC model for (a) 10 years; (b) 20 years; (c) 30 years; (d) 40 years; (e) 50 years; and (f) Digital elevation model (DEM).

**Table 4.** Soil organic carbon stock in different land cover

Land cover	Area	Years					
		0	10	20	30	40	50
	%	Mg ha <sup>-1</sup>					
Tree cover	10909 (5.1)	112.19	119.44	120.60	120.65	120.49	120.30
Grassland	157379 (74.4)	149.62	147.74	144.89	142.36	140.06	137.94
Bare/sparse vegetation	4243 (2.0)	177.16	173.02	168.56	164.91	161.72	158.81
Cropland	38843 (18.5)	101.53	104.66	105.10	105.19	105.21	105.22
Cropland + Manure		101.53	204.53	208.83	211.29	213.23	214.94

To determine the benefits of incorporating 1 Mg of manure, we calculated ratios by dividing the values obtained from the model simulation by the values without application when the application occurs. Spatial distribution of ratio values in the basin facilitates the identification of the specific areas with the highest levels of positive changes (Figure 4). After tabulating data from raster maps, a comprehensive statistical summary highlights a significant 24 percent profit growth in the last year assessed. It reveals a continuous upward trend in mean values, with a constant growth range of 1 to 2 percent.

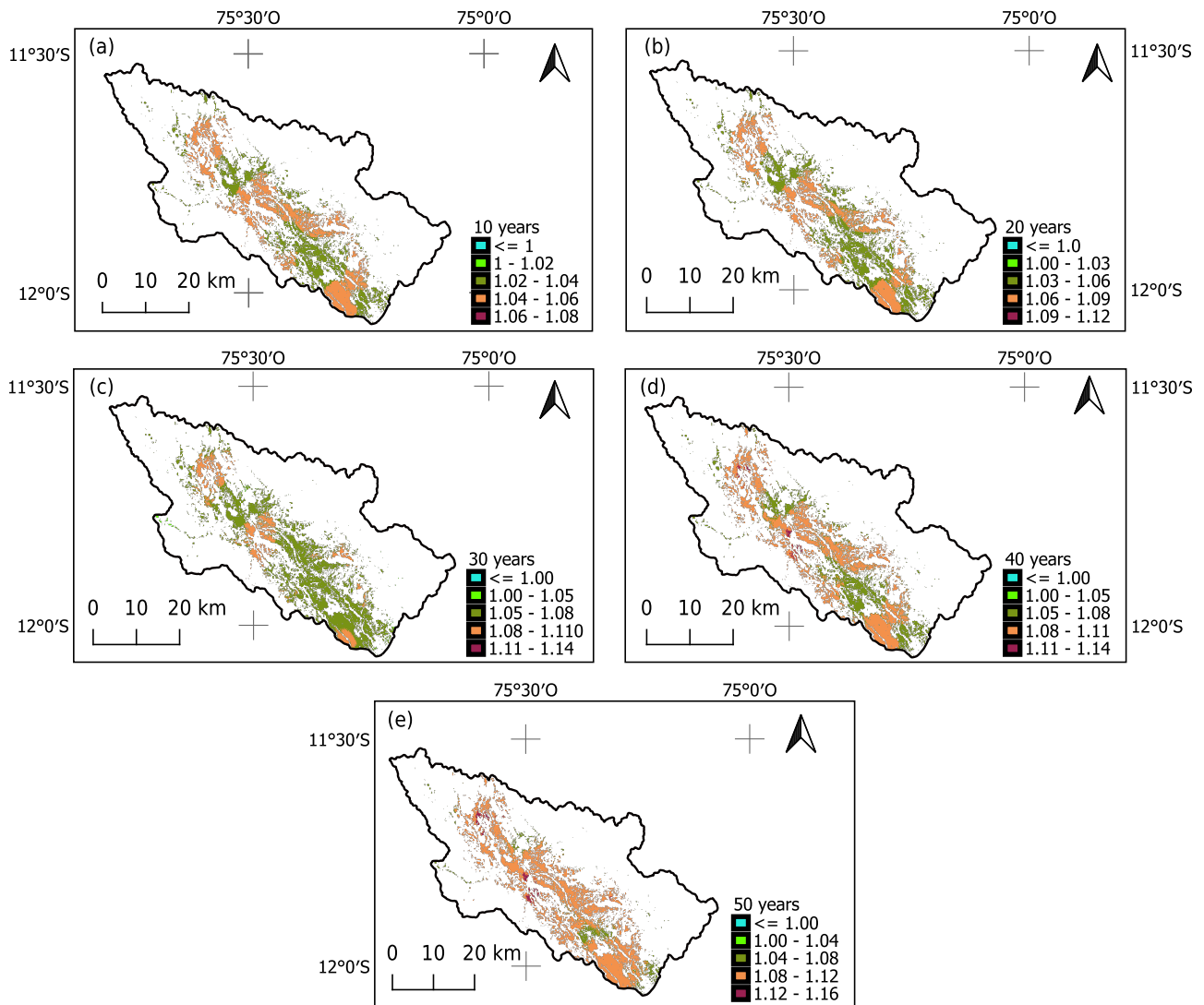


**Figure 4.** Spatial distribution of variation rates after applying 1 Mg of manure for (a) 10 years, (b) 20 years, (c) 30 years, (d) 40 years, and (e) 50 years in cropland areas.

## DISCUSSION

All soil samples were classified as mineral materials (Soil Survey Staff, 2022), with organic carbon contents less than 12 %. Carbon sequestration capacity of mineral soils is based on the organic-mineral association, where carbon is sorbed onto the surface of clay minerals (Rodríguez-Albarracín et al., 2023). The high-altitude Peruvian Andean Cordillera is characterized by high accumulations of organic carbon, and the clay fraction is predominantly composed of kaolinite, quartz, and illite minerals (Lama-Isminio et al., 2024). The high clay content observed in our study (Table 2) suggests significant potential for carbon sequestration. Soil organic carbon typically exhibits an aggregated spatial distribution and can be effectively modeled using geostatistical techniques (Han et al., 2010). Compared to other studies (Chabala et al., 2017; Zhang et al., 2021), the spatial structure of soil organic carbon in our study is more extensive, with hotspots of high concentration located in the central region.

RothC model is widely used in predicting SOC changes and has been implemented in multiple programming languages, such as C++ (Dechow et al., 2019), Python (Coleman et al., 2024), and R (Sierra et al., 2014). By utilizing the SoilR package in R, we can merge soil, climate, and remote sensing datasets to estimate changes in soil organic

carbon stocks over different timeframes and environmental situations. Soil organic carbon rates over 45 years increased from 0.1 to 2.6 Mg ha<sup>-1</sup> yr<sup>-1</sup> with transitioning from traditional tillage to conservation one (González-Molina et al., 2017), for 30 years with different slope gradients and land types, showing higher SOC in grass/fallow land than cultivated land and plantation forest (Geremew et al., 2024). Other studies have shown that SOC values were higher in natural and mixed forest land use (Amanuel et al., 2018). Using the RothC model, we identified areas with sparse vegetation that exhibited permanently high SOC values during the 50 years projected, prompting us to assess terrain conditions characterized by high elevations and steep slopes (Figure 3). The estimated extent of the bare-sparse area is much smaller than the uncertainty associated with the ESA 2021 Land Cover product (Zanaga et al., 2022), which raises doubts about the accuracy of this data for determining coverage. It is suggested that the coverage be expanded to include a larger area of the surrounding land.

Despite limitations like its exclusion of soil pH effects on soil carbon, limitations in waterlogged conditions (Geremew et al., 2024), and uses total C inputs instead of differentiating between above- and below-ground inputs (Nemo et al., 2017), the RothC model demonstrates considerable predictive power. Local calibration efforts have only marginally improved its accuracy, increasing it from 78 to 98 % (Jebari et al., 2021), demonstrating the model's inherent strength and robustness even in its unmodified form. This is particularly critical given the severely limited investment in science within the Andean region (Valdez et al., 2024). This scarcity of funding hinders the implementation of long-term research initiatives required to calibrate RothC, especially in geographically challenging areas like the Peruvian Andes. A comparison of RothC estimates for 2023 with limited data from 1975 revealed no statistically significant differences. While this concordance suggests some degree of reliability for RothC estimates in the area, the limited number of historical data points warrants caution in extrapolating these findings.

RothC model has demonstrated that soil carbon losses increase under climate change scenarios (Xu et al., 2011). Soil management and conservation practices focused on improving soil structure and applying organic matter can restore degradation and increase soil carbon stocks (Chatterjee et al., 2021). While manure applications between 7 (Justo and Otiniano, 2021) and 20 Mg ha<sup>-1</sup> (Chirinos-Peinado et al., 2020) have been shown to improve agricultural production in Peruvian soils, and RothC simulations suggest that an average application of 9 Mg ha<sup>-1</sup> can offset carbon losses (Kaushal et al., 2023). The Mantaro Valley has monetary poverty levels that rise to 30.4 % (Aliaga et al., 2022), and the agricultural population of Peru that applies adequate doses of manure amounts to only 25.18 % of the total agricultural units (Instituto Nacional de Estadística e Informática - INEI, 2012). This reality makes it impossible for farmers in the study zone to apply amounts of manure between 7 to 20 Mg ha<sup>-1</sup>. Our results show that over a 50-year period, doses of 1 Mg per hectare of manure application offset carbon losses from grassland and bare-sparse land (Table 4), and when observing the spatial distribution of their ratios, there is a notable increase as the simulation progresses in time (Figure 4).

Potatoes are a major crop in the Mantaro Valley, with production costs ranging from 3000 to 4000 USD, per agricultural campaign (Galarza, 2020). Utilizing a single Mg of manure, with costs ranging from \$ 100 to \$ 270, constitutes less than 10 % of the overall agricultural campaign costs, yet it promotes enhanced crop yields (Otieno and Mageto, 2021). Product availability is not a limiting factor, given the substantial population of bovine, sheep, alpaca, and swine producers (*Instituto Nacional de Estadística e Informática* - INEI, 2012) distributed uniformly across the study area. To facilitate the adoption of these sustainable practices, it is crucial for local government agencies to actively engage with and empower farmers, enabling them to achieve low-carbon agriculture while maintaining adequate yields.

## CONCLUSIONS

The study employed the RothC model to evaluate soil carbon storage in Andean croplands, revealing that applying 1 Mg of manure can increase carbon storage by up to 24 % over a 50-year period. This serves as a crucial reference for future projects focused on enhancing sustainable land management practices for Andean agriculture, particularly regarding soil health and carbon sequestration.

Using manure on croplands can offset the loss of soil organic carbon in other areas, like grasslands, and increase carbon sequestration. Taking this integrated approach is important for managing carbon across the entire basin.

RothC model in one R programming language environment using SoilR package, join to use geostatistical techniques, establishes a solid framework for future studies on soil organic carbon in similar environments.

This study positively addressed the existing knowledge gap regarding SOC dynamics in the understudied Peruvian Andean region, opening the possibility that further research could explore the economic and practical feasibility of manure application at different scale approach, as well as other potential management practices.

## DATA AVAILABILITY

The data will be provided upon request.

## FUNDING

This research was funded by INIA project “Mejoramiento de los servicios de investigación y transferencia tecnológica en el manejo y recuperación de suelos agrícolas degradados y aguas para riego en la pequeña y mediana agricultura en los departamentos de Lima, Áncash, San Martín, Cajamarca, Lambayeque, Junín, Ayacucho, Arequipa, Puno y Ucayali”, CUI 2487112.



## ACKNOWLEDGMENTS

The authors are grateful for the collaboration of Jhoselin Ospina and Miguel Mendoza from E.E.A. Santa Ana - INIA, as well as the support of Jimmy Espíritu in the laboratory in the C.E. La Molina—INIA.

## AUTHOR CONTRIBUTIONS

**Conceptualization:**  Carlos Carbajal (lead).

**Data curation:**  Carlos Carbajal (equal) and  Carlos Mestanza (equal).

**Formal analysis:**  Carlos Carbajal (equal) and  Carlos Mestanza (equal).

**Investigation:**  Carlos Carbajal (equal) and  Jesús Vera (equal).

**Methodology:**  Carlos Carbajal (equal) and  Carlos Mestanza (equal).

**Resources:**  Jesús Vera (lead).

**Software:**  Carlos Carbajal (lead).

**Validation:**  Carlos Mestanza (lead).

**Visualization:**  Carlos Carbajal (lead).

**Writing - review & editing:**  Samuel Pizarro (lead).

**Writing—Original Draft:**  Carlos Carbajal (equal) and  Carlos Mestanza (equal).

## REFERENCES

- Alavi-Murillo G, Diels J, Gilles J, Willems P. Soil organic carbon in Andean high-mountain ecosystems: importance, challenges, and opportunities for carbon sequestration. *Reg Environ Change*. 2022;22:128. <https://doi.org/10.1007/s10113-022-01980-6>
- Aliaga R, Ríos-Carmenado I, Howard FSM, Espinoza SC, Cristóbal AH. Integration of the principles of responsible investment in agriculture and food systems CFS-RAI from the local action groups: Towards a model of sustainable rural development in Jauja, Peru. *Sustainability*. 2022;14:9663. <https://doi.org/10.3390/su14159663>
- Amanuel W, Yimer F, Karlton E. Soil organic carbon variation in relation to land use changes: the case of Birr watershed, upper Blue Nile River Basin, Ethiopia. *J Ecology Environ*. 2018;42:16. <https://doi.org/10.1186/s41610-018-0076-1>
- Avadí A. Environmental assessment of the Ecuadorian cocoa value chain with statistics-based LCA. *Int J Life Cycle Assess*. 2023;28:1495-515. <https://doi.org/10.1007/s11367-023-02142-4>
- Bivand R, Keitt T, Rowlingson B. rgdal: Bindings for the ‘geospatial’ data abstraction library. Package rgdal; 2023. Available from: <https://CRAN.R-project.org/package=rgdal> .
- Bradford MA, Carey CJ, Atwood L, Bossio D, Fenichel EP, Gennet S, Fargione J, Fisher JRB, Fuller E, Kane DA, Lehmann J, Oldfield EE, Ordway EM, Rudek J, Sanderman J, Wood SA. Soil carbon science for policy and practice. *Nat Sustain*. 2019;2:1070-2. <https://doi.org/10.1038/s41893-019-0431-y>
- Canaza D, Calizaya E, Chambi W, Calizaya F, Mindani C, Cuentas O, Caira C, Huacani W. Spatial distribution of soil organic carbon in relation to land use, based on the weighted overlay technique in the high andean ecosystem of Puno—Peru. *Sustainability*. 2023;15:10316. <https://doi.org/10.3390/su151310316>
- Castro A, Arriaga CD, Laura W, Saucedo FC, Avalos G, López C, Villena D, Valdez M, Urbiola J, Trebejo I, Menis L, Sanchez DEM. Climas del Perú: Mapa de clasificación climática nacional. Perú: Servicio Nacional de Meteorología e Hidrología del Perú; 2021. Available from: <https://hdl.handle.net/20.500.12542/1336>
- Chabala LM, Mulolwa A, Lungu O. Application of ordinary kriging in mapping soil organic carbon in Zambia. *Pedosphere*. 2017;27:338-43. [https://doi.org/10.1016/S1002-0160\(17\)60321-7](https://doi.org/10.1016/S1002-0160(17)60321-7)
- Chatterjee S, Ghosh S, Pal P. Soil carbon restoration through conservation agriculture. In: Rhodes ER, Naser H, editors. *Natural resources management and biological sciences*. London: IntechOpen; 2021. <https://doi.org/10.5772/intechopen.93006>
- Chirinos-Peinado D, Castro-Bedriñana J, Lara-Schwartz P. Biofortification of the Ryegrass (*Lolium multiflorum* L.) with chicken manure compost in the central sierra of Peru. *Adv Sci Technol Eng Syst J*. 2020;5:418-23. <https://doi.org/10.25046/aj050153>
- Coleman K, Jenkinson DS. RothC-26.3 - A Model for the turnover of carbon in soil. In: Powlson DS, Smith P, Smith JU, editors. *Evaluation of soil organic matter models*. Berlin, Heidelberg: Springer Berlin Heidelberg; 1996. p. 237-46. [https://doi.org/10.1007/978-3-642-61094-3\\_17](https://doi.org/10.1007/978-3-642-61094-3_17)
- Coleman K, Milne A, Prout J. Python version of RothC Official Rothamsted Research Release. Version v1.0.0. Zenodo; 2024. <https://doi.org/10.5281/zenodo.10732265>
- Conrad O, Bechtel B, Bock M, Dietrich H, Fischer E, Gerlitz L, Wehberg J, Wichmann V, Böhrner J. System for Automated Geoscientific Analyses (SAGA) v. 2.1.4. *Geosci Model Dev*. 2015;8:1991-2007. <https://doi.org/10.5194/gmd-8-1991-2015>
- Cuellar-Bautista J, Medina-Hinostroza T. Agrobiodiversidad, género y cambio climático en la cuenca del río Mantaro. *Tecnología y Sociedad*. 2009;16:83-99. Available from: <https://repositorio.inia.gob.pe/handle/20.500.12955/556>.

- Dechow R, Franko U, Kätterer T, Kolbe H. Evaluation of the RothC model as a prognostic tool for the prediction of SOC trends in response to management practices on arable land. *Geoderma*. 2019;337:463-78. <https://doi.org/10.1016/j.geoderma.2018.10.001>
- Diaz CA, Baluganic E, Zamora-Ledezma E, Hamelin L. Strengthening the bioeconomy in tropical countries while preserving soil organic carbon stocks by recycling recalcitrant coproducts: A case study for Ecuador. In: EGU23, the 25th EGU General Assembly, held 23-28 April, 2023 in Vienna, Austria and Online. 2023; p. EGU-6867. <https://doi.org/10.5194/egusphere-egu23-6867>
- Falloon P, Smith P, Coleman K, Marshall S. Estimating the size of the inert organic matter pool from total soil organic carbon content for use in the Rothamsted carbon model. *Soil Biol Biochem*. 1998;30:1207-11. [https://doi.org/10.1016/S0038-0717\(97\)00256-3](https://doi.org/10.1016/S0038-0717(97)00256-3)
- Food and Agriculture Organization of the United Nations - FAO. Global soil organic carbon sequestration potential map - GSOCseq v.1.1. Technical report. Rome: FAO; 2022
- Fick SE, Hijmans RJ. WorldClim 2: New 1-km spatial resolution climate surfaces for global land areas. *Int J Climatol*. 2017;37:4302-15. <https://doi.org/10.1002/joc.5086>
- Galarza WMF. Estrategias de comercialización para mejorar la rentabilidad de la papa única en el Distrito de Huasahuasi, Tarma, Junín 2019 [thesis]. Lima, Perú: Universidad Norbert Wiener; 2020.
- Geremew B, Tadesse T, Bedadi B, Gollany HT, Tesfaye K, Aschalew A, Tilaye A, Abera W. Evaluation of RothC model for predicting soil organic carbon stock in north-west Ethiopia. *Environ Chall*. 2024;15:100909. <https://doi.org/10.1016/j.envc.2024.100909>
- González-Molina L, Moreno-Pérez EC, Báez-Pérez A. Simulation of soil organic carbon changes in Vertisols under conservation tillage using the RothC model. *Sci Agric*. 2017;74:235-41. <https://doi.org/10.1590/1678-992X-2015-0487>
- Gower JC. A general coefficient of similarity and some of its properties. *Biometrics*. 1971;27:857. <https://doi.org/10.2307/2528823>
- Han F, Hu W, Zheng J, Du F, Zhang X. Spatial variability of soil organic carbon in a catchment of the Loess Plateau. *Acta Agr Scand B - S*. 2010;60:136-43. <https://doi.org/10.1080/09064710902721354>
- Hengl T, Jesus JM, Heuvelink GBM, Gonzalez MR, Kilibarda M, Blagotić A, Shangguan W, Wright MN, Geng X, Bauer-Marschallinger B, Guevara MA, Vargas R, MacMillan RA, Batjes NH, Leenaars JGB, Ribeiro E, Wheeler I, Mantel S, Kempen B. SoilGrids250m: Global gridded soil information based on machine learning. *PLoS ONE*. 2017;12:e0169748. <https://doi.org/10.1371/journal.pone.0169748>
- Hijmans RJ. raster: Geographic data analysis and modeling. Package raster; 2024. <https://doi.org/10.32614/CRAN.package.raster>
- Instituto Nacional de Estadística e Informática - INEI. Censo nacional agropecuario (CENAGRO). Plataforma Nacional de Datos Abiertos; 2012. Available from: <https://www.datosabiertos.gob.pe/>.
- International Organization for Standardization - ISO. Soil quality - Determination of dry bulk density; 2017. (ISO 11272:2017).
- International Organization for Standardization - ISO. Soil quality - Determination of organic and total carbon after dry combustion; 1996. (ISO 10694:1996).
- IUSS Working Group WRB. World reference base for soil resources 2006, first update 2007: International soil classification system for naming soils and creating legends for soil maps. Rome: Food and Agriculture Organization of the United Nations; 2007. (World Soil Resources Reports, 103).
- Jebari A, Álvaro-Fuentes J, Pardo G, Almagro M, Del Prado A. Estimating soil organic carbon changes in managed temperate moist grasslands with RothC. *PLoS ONE*. 2021;16:e0256219. <https://doi.org/10.1371/journal.pone.0256219>
- Justo EB, Otiniano AJ. Efecto de la materia orgánica en el cultivo de palto variedad Fuerte en Moquegua, Perú. *Idesia*. 2021;39:111-9. <https://doi.org/10.4067/S0718-34292021000400111>

- Kaushal R, Panwar P, Durai J, Tomar JMS, Mandal D, Dogra P, Gupta A, Reza S, Singh C, Madhu M. Simulating SOC dynamics under different temperature regimes and FYM addition in bamboo species using RothC-Model. *Forests*. 2023;14:722. <https://doi.org/10.3390/f14040722>
- Lama-Isminio AD, Schaefer CEGR, Amaral EF, Lopes DV, Rocha-Francelino M, Osório-Senra E. Soil-Landform interplays from the Highlands of the Eastern Andes Cordillera to the lowlands of the Peruvian Amazon. *Catena*. 2024;244:108248. <https://doi.org/10.1016/j.catena.2024.108248>
- Lin Z, Lu X, Xu Y, Sun W, Yu Y, Zhang W, Mishra U, Kuzyakov Y, Wang G, Qin Z. Increased straw return promoted soil organic carbon accumulation in China's croplands over the past 40 years. *Sci Total Environ*. 2024;945:173903. <https://doi.org/10.1016/j.scitotenv.2024.173903>
- McBratney AB, Stockmann U, Angers DA, Minasny B, Field DJ. Challenges for soil organic carbon research. In: Hartemink AE, McSweeney K, editors. *Soil carbon*. Cham: Springer International Publishing; 2014. p. 3-16. [https://doi.org/10.1007/978-3-319-04084-4\\_1](https://doi.org/10.1007/978-3-319-04084-4_1)
- Mousavi A, Karimi A, Maleki S, Safari T, Taghizadeh-Mehrjardi R. Digital mapping of selected soil properties using machine learning and geostatistical techniques in Mashhad plain, northeastern Iran. *Environ Earth Sci*. 2023;82:234. <https://doi.org/10.1007/s12665-023-10919-x>
- Murphy BS. *PyKriging: Kriging Toolkit for Python*; 2024.
- Nachshon U. Soil degradation processes: It's time to take our head out of the sand. *Geosciences*. 2020;11:2. <https://doi.org/10.3390/geosciences11010002>
- Nemo KK, Coleman K, Dondini M, Goulding K, Hastings A, Jones MB, Leifeld J, Osborne B, Saunders M, Scott T, Teh YA, Smith P. Soil organic carbon (SOC) equilibrium and model initialisation methods: An application to the Rothamsted Carbon (RothC) model. *Environ Model Assess*. 2017;22:215-29. <https://doi.org/10.1007/s10666-016-9536-0>
- Otieno HMO, Mageto EK. A review on yield response to nitrogen, potassium and manure applications in potato (*Solanum tuberosum* L.) production. *Arch Agric Environ Sci*. 2021;6:80-6. <https://doi.org/10.26832/24566632.2021.0601011>
- Pedregosa F, Varoquaux G, Gramfort A, Michel V, Thirion B, Grisel O, Blondel M, Prettenhofer P, Weiss R, Dubourg V. Scikit-learn: Machine learning in python. *J Mach Learn Res*. 2011;12:2825-30. <https://doi.org/10.48550/arXiv.1201.0490>
- R Development Core Team. R: A language and environment for statistical computing. Vienna, Austria: R Foundation for Statistical Computing; 2023. Available from: <http://www.R-project.org/>.
- Ramesh T, Bolan NS, Kirkham MB, Wijesekara H, Kanchikerimath M, Rao CS, Sandeep S, Rinklebe J, Ok YS, Choudhury BU, Wang H, Tang C, Wang X, Song Z, Freeman li OW. Soil organic carbon dynamics: Impact of land use changes and management practices: A review. *Adv Agron*. 2019;156:1-107. <https://doi.org/10.1016/bs.agron.2019.02.001>
- Riggers C, Poeplau C, Don A, Frühauf C, Dechow R. How much carbon input is required to preserve or increase projected soil organic carbon stocks in German croplands under climate change? *Plant Soil*. 2021;460:417-33. <https://doi.org/10.1007/s11104-020-04806-8>
- Rodríguez-Albarracín HS, Demattê JAM, Rosin NA, Contreras AED, Silvero NEQ, Cerri CEP, Mendes WS, Tayebi M. Potential of soil minerals to sequester soil organic carbon. *Geoderma*. 2023;436:116549. <https://doi.org/10.1016/j.geoderma.2023.116549>
- Roudier P. *clhs: a R package for conditioned Latin hypercube sampling*. Package clhs; 2011. <https://doi.org/10.32614/CRAN.package.clhs>
- Roudier P, Beaudette D, Hewitt A. A conditioned Latin hypercube sampling algorithm incorporating operational constraints. In: Minasny B, Malone BP, McBratney AB, editors. *Digital soil assessments and beyond: Proceedings of the 5th Global Workshop on Digital Soil Mapping*. London: CRC Press; 2012. p. 227-32. <https://doi.org/10.1201/b12728-46>
- Rumpel C, Amiraslani F, Chenu C, Cardenas MG, Kaonga M, Koutika L-S, Ladha J, Madari B, Shirato Y, Smith P, Soudi B, Soussana J-F, Whitehead D, Wollenberg E. The 4p1000 initiative: Opportunities, limitations and challenges for implementing soil organic carbon sequestration as a sustainable development strategy. *Ambio*. 2020;49:350-60. <https://doi.org/10.1007/s13280-019-01165-2>

- Running S, Zhao M. MODIS/Terra Net Primary Production Gap-Filled Yearly L4 Global 500 m SIN Grid V061. Washington, DC: Nasa Eosdis Land Processes Daac; 2021. <https://doi.org/10.5067/MODIS/MOD17A3HGF.061>
- Siddique KHM, Bolan N, Rehman A, Farooq M. Enhancing crop productivity for recarbonizing soil. *Soil Till Res.* 2024;235:105863. <https://doi.org/10.1016/j.still.2023.105863>
- Sierra CA, Müller M. A general mathematical framework for representing soil organic matter dynamics. *Ecol Monogr.* 2015;85:505-24. <https://doi.org/10.1890/15-0361.1>
- Sierra CA, Müller M, Trumbore SE. Modeling radiocarbon dynamics in soils: SoilR version 1.1. *Geosci Model Dev.* 2014;7:1919-31. <https://doi.org/10.5194/gmd-7-1919-2014>
- Soil Survey Staff. Keys to soil taxonomy. 13th ed. Washington, DC: United States Department of Agriculture, Natural Resources Conservation Service; 2022.
- Valdez JW, Vergara LC, Orihuela G, Fernandez M. Overcoming the Tropical Andes publication divide: Insights from local researchers on challenges and solutions. *PLoS ONE.* 2024;19:e0306189. <https://doi.org/10.1371/journal.pone.0306189>
- Van Rossum G, Drake Jr FL. Python reference manual. Amsterdam: Centrum voor Wiskunde en Informatica; 1995.
- Wang S, Xu L, Adhikari K, He N. Soil carbon sequestration potential of cultivated lands and its controlling factors in China. *Sci Total Environ.* 2023;905:167292. <https://doi.org/10.1016/j.scitotenv.2023.167292>
- Weihermüller L, Graf A, Herbst M, Vereecken H. Simple pedotransfer functions to initialize reactive carbon pools of the RothC model. *Eur J Soil Sci.* 2013;64:567-75. <https://doi.org/10.1111/ejss.12036>
- Xu X, Liu W, Kiely G. Modeling the change in soil organic carbon of grassland in response to climate change: Effects of measured versus modelled carbon pools for initializing the Rothamsted Carbon model. *Agr Ecosyst Environ.* 2011;140:372-81. <https://doi.org/10.1016/j.agee.2010.12.018>
- Zanaga D, Van De Kerchove R, Daems D, Keersmaecker W, Brockmann C, Kirches G, Wevers J, Cartus O, Santoro M, Fritz S, Lesiv M, Herold M, Tsendbazar N-E, Xu P, Ramoino F, Arino O. ESA WorldCover 10 m 2021 v200; 2022b. <https://doi.org/10.5281/ZENODO.7254221>
- Zhang P, Wang Y, Sun H, Qi L, Liu H, Wang Z. Spatial variation and distribution of soil organic carbon in an urban ecosystem from high-density sampling. *Catena.* 2021;204:105364. <https://doi.org/10.1016/j.catena.2021.105364>
- Zimmermann M, Leifeld J, Schmidt MWI, Smith P, Fuhrer J. Measured soil organic matter fractions can be related to pools in the RothC model. *Eur J Soil Sci.* 2007;58:658-67. <https://doi.org/10.1111/j.1365-2389.2006.00855.x>
- Zomer RJ, Xu J, Trabucco A. Version 3 of the c. *Sci Data.* 2022;9:409. <https://doi.org/10.1038/s41597-022-01493-1>